Green Chemistry

COMMUNICATION

View Article Online
View Journal

Cite this: DOI: 10.1039/d6gc00098c

Received 6th January 2026,
Accepted 19th March 2026

DOI: 10.1039/d6gc00098c

rsc.li/greenchem

Upcycling poly(ε-caprolactone) into azepane *via* reductive ammonolysis over a titanium oxide-supported platinum catalyst

Daratu E. K. Putri, [a,b] Katsumasa Sakoda,[a] Yoshiki Takamoto,[a] Sho Yamaguchi, [a,c] Takato Mitsudome [a,d] and Tomoo Mizugaki [a,d,e]*

Upcycling aliphatic polyesters into nitrogen-containing heterocycles offers an emerging route to valuable chemicals from plastic waste. Herein, we report the first demonstration of direct transformation of poly(ε-caprolactone) (PCL) into azepane (AZP), a bioactive seven-membered N-heterocycle relevant to pharmaceutical synthesis. A titanium oxide-supported platinum catalyst (Pt/TiO_2) efficiently promotes the transformation, affording AZP in 75% yield, and exhibits robust reusability. Spectroscopic analyses and control experiments reveal that TiO_2 facilitates the initial depolymerization of PCL *via* vacancy-associated Lewis acid sites, while electron-rich Pt nanoparticles (NPs) promote H_2 dissociation. The synergistic interplay between Pt and TiO_2 enables the sequential depolymerization and hydrogenation of PCL, leading to the highly selective formation of AZP. This catalytic platform provides a practical and reusable route for plastic valorization, enabling sustainable access to bioactive nitrogen heterocycles from polymeric feedstocks.

Green foundation

1. This work advances plastic upcycling by providing the first demonstration of direct conversion of PCL into AZP, a nitrogen-containing cyclic compound with pharmaceutical relevance.
2. The Pt/TiO_2 catalyst enables the direct transformation of PCL into AZP with high activity and reusability, simplifying the reaction sequence and avoiding intermediate isolation.
3. The use of a reusable heterogeneous catalyst in a single-step transformation highlights the practicality of this upcycling approach.

The rapid growth of plastic has created a persistent environmental challenge, as most plastic waste is either accumulated in the environment or incinerated,[1,2] causing substantial ecological harm.[3,4] Although biodegradable polymers have been developed as alternatives, their slow degradation and conversion primarily into CO_2 limit material recovery.[5,6] Chemical recycling and upcycling have therefore gained attention as promissing approaches to address plastic waste.[7–10] Despite these advances, their broader implementation remains limited by the structural complexity of plastics, high energy demands, and challenges in selectivity and solvation.[11,12] Developing new upcycling methods to overcome these barriers is thus essential.

PCL, produced industrially through the ring-opening polymerization of ε-caprolactone (CLO), is widely used in biomedical applications, including drug delivery systems, tissue-engineering scaffolds, and wound healing.[13] Catalytic depolymerization of PCL back to CLO has been extensively explored (Scheme 1-I).[14,15] In addition, chemical recycling systems involving depolymerization to methyl 6-hydroxycaproate[16] or 1,6-hexanediol,[17–19] followed by re-polymerization, have been developed (Scheme 1-I). In contrast, upcycling strategies that transform PCL into structurally distinct, higher-value chemicals remain rare. To date, reported examples are only limited to Ru-catalysed aminolysis affording 6-aminocaproic acid and ε-caprolactam (CLA),[20] as well as a Pt-catalysed oxidative degradation into adipic acid (Scheme 1-II).[21] Given these limitations, developing new upcycling strategies is essential.

Cycloaddition strategies to seven-membered N-heterocycles remain limited, and enthalpic/entropic penalties hinder

[a]*Department of Materials Engineering Science, Graduate School of Engineering Science, The University of Osaka, 1-3 Machikaneyama, Toyonaka, Osaka 560-8531, Japan. E-mail: mizugaki.tomoo.es@osaka-u.ac.jp*
[b]*Departemen Kimia, Fakultas Matematika dan Ilmu Pengetahuan Alam, Universitas Negeri Malang, Jl. Semarang 5, Lowokwaru, Malang 65145, Indonesia*
[c]*Graduate School of Engineering, Kobe University, Kobe, Hyogo 657-8501, Japan*
[d]*Innovative Catalysis Science Division, Institute for Open and Transdisciplinary Research Initiatives (ICS-OTRI), The University of Osaka, Suita, Osaka 565-0871, Japan*
[e]*Research Center for Solar Energy Chemistry, Graduate School of Engineering Science, The University of Osaka, 1-3 Machikaneyama, Toyonaka, Osaka 560-8531, Japan*

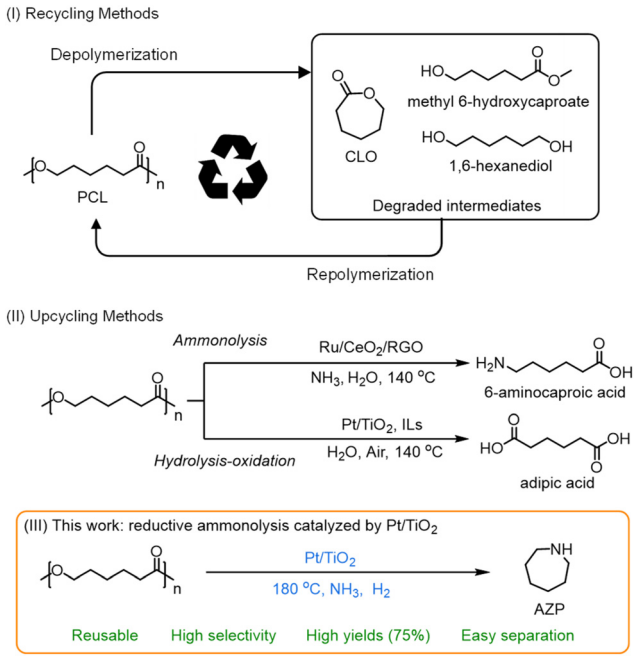

Scheme 1 (I) Chemical recycling of PCL *via* CLO,[14,15] 6-hydroxycaproate,[16] and 1,6-hexanediol.[17–19] (II) Upcycling of PCL to produce 6-aminocaproic acid[20] and adipic acid.[21] (III) Upcycling of PCL to produce AZP (this work).

robust direct construction.[22,23] Moreover, AZP lacks convenient precursors, and its synthesis relies on multistep preparation of linear intermediates, followed by cyclization.[24] Against this backdrop, the reductive ammonolysis of PCL offers a direct entry to AZP from an abundant feedstock.

Herein, we present for the first time the direct upcycling of PCL into AZP under reductive ammonolysis conditions (Scheme 1-III). This transformation is achieved using a titanium oxide supported Pt (Pt/TiO_2). AZP is a nitrogen-containing heterocycle with antidiabetic, anticancer, and antiviral potential.[25] This protocol provides a sustainable strategy for PCL upcycling, enabling direct access to a high-value nitrogen-containing heterocycle with broad application potential.

The catalytic performance of various supported metal nanoparticles was evaluated for the reductive ammonolysis of PCL under H_2 (4.0 MPa) and NH_3 (0.7 MPa) at 180 °C (Table 1). Among the catalysts tested, Pt/TiO_2 exhibited the highest activity, affording AZP in 18% yield after 6 h together with the formation of CLA (Table 1, entry 1). Upon prolonging the reaction time from 6 h to 25 h, the yield of AZP improved to 75% (Table 1, entry 2). In contrast, catalysts with other platinum-group metals (Rh, Ru, and Pd) were ineffective under identical conditions (Table 1, entries 3–5). Pt catalysts supported on Al_2O_3, ZrO_2, or CeO_2 showed much lower activity for AZP formation (Table 1, entries 6–8). Bare TiO_2 also exhibited no catalytic activity toward AZP formation (Table 1, entry 9). These results indicate that the combination of Pt and TiO_2 is crucial for promoting the reductive ammonolysis of PCL into AZP.

Table 1 Upcycling of PCL with NH_3 to AZP over various supported metal catalysts[a]

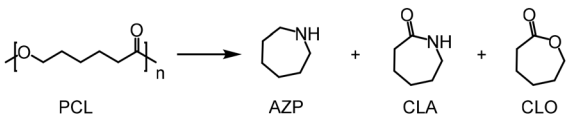

		Yield[b] [%]		
Entry	Catalyst	AZP	CLA	CLO
1	Pt/TiO_2	18	24	0
2[c]	Pt/TiO_2	75	0	0
3	Rh/TiO_2	0	18	0
4	Ru/TiO_2	0	6	0
5	Pd/TiO_2	0	5	0
6	Pt/Al_2O_3	8	17	6
7	Pt/ZrO_2	0	11	0
8	Pt/CeO_2	0	9	0
9	TiO_2	0	0	6

[a] Reaction conditions: catalyst (0.15 g, Pt: 8 mol%), PCL (0.5 mmol), *n*-heptane (10 mL), 180 °C, NH_3 (0.7 MPa), H_2 (4 MPa), 6 h. [b] Yield was determined by gas chromatography-flame ionization detection (GC-FID) using an internal standard for analysis and calculated based on PCL. [c] 25 h.

The reusability of Pt/TiO_2 was investigated. After the reaction, the catalyst was recovered by centrifugation, calcined at 400 °C, and reused in subsequent runs (Fig. 1). The Pt/TiO_2 catalyst maintained high activity and selectivity over four consecutive runs with negligible loss of performance. Inductively coupled plasma-atomic emission spectrometry analysis revealed that the Pt loading amounts remained unchanged between the fresh and used catalysts, confirming that Pt leaching was insignificant during the reaction (Table S2). In the 5th cycle, a decrease in AZP yield to 44% was observed, accompanied by the formation of CLA as a by-product.

This PCL-to-AZP conversion offers several green-chemistry advantages. It proceeds without stoichiometric activation of reagents and furnishes a pharmaceutically relevant N-heterocycle with water as the sole stoichiometric by-product. Using an AZP-only product boundary and assuming solvent

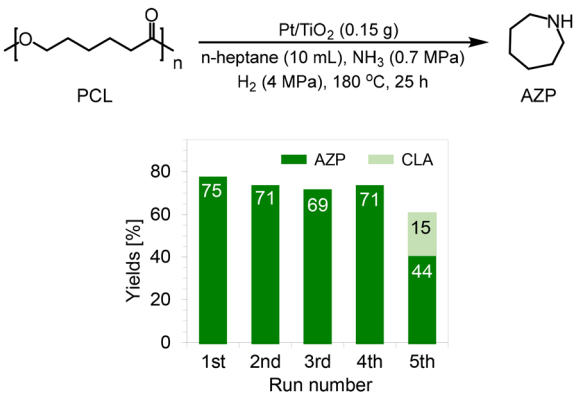

Fig. 1 Reusability of the Pt/TiO_2 catalyst for reductive ammonolysis of PCL.

recovery, the calculated atom economy and *E*-factor are 73% and 0.48, respectively (SI, Section S5).

To clarify whether the catalyst structure contributes to its high performance in AZP formation, Pt/TiO_2 was treated under reaction conditions and characterized (see the SI for details). The powder X-ray diffraction (XRD) pattern of the treated Pt/TiO_2 showed diffraction peaks assigned to anatase TiO_2 and metallic Pt^0 (Fig. 2a). Transmission electron microscopy (TEM) revealed the presence of Pt nanoparticles with a mean diameter of 2.7 nm dispersed on the TiO_2 surface (Fig. 2b). A high-resolution TEM image showed lattice fringes with a *d*-spacing of approximately 0.20 nm, corresponding to the (200) plane of face-centered cubic Pt NPs (Fig. S3). In addition, Pt L_3-edge X-ray absorption near-edge structure (XANES) measurements were performed to reveal the electronic state of Pt species in Pt/TiO_2 (Fig. 2c). The white line intensity of the Pt L_3-edge XANES spectrum of the treated Pt/TiO_2 catalyst was similar to that of Pt foil, suggesting the presence of metallic Pt^0. To further investigate the surface electronic state of Pt, X-ray photoelectron spectroscopy (XPS) analysis was carried out (Fig. 2d). The Pt $4f_{7/2}$ peak of the treated Pt/TiO_2 was observed at 70.7 eV, consistent with metallic Pt^0. Notably, this binding energy is slightly lower than that in the bulk Pt phase (71.4 eV), indicating electron density enrichment at the Pt nanoparticles. This observation is consistent with metal–support interaction between TiO_2 and Pt nanoparticles,[26,27] which may contribute to the catalyst's stability in PCL transformation. Such electron-rich Pt^0 species are also likely to facilitate H_2 dissociation.[28,29]

The role of the TiO_2 support in PCL upcycling was also investigated. NH_3-temperature-programmed desorption (NH_3-TPD) analysis revealed that Pt/TiO_2 treated under reaction conditions possessed significantly stronger acid sites compared to other metal oxides tested (Fig. S8a). Electron spin resonance (ESR) spectroscopy further confirmed the presence of oxygen vacancies ($g \approx 2.003$), which are associated with enhanced surface acidity (Fig. S8b and S9).[30–32] *In situ* pyridine-FTIR measurements provided complementary evidence, revealing an increased Lewis-to-Brønsted ratio in the treated Pt/TiO_2 (Fig. S10). The oxygen-vacancy sites on the TiO_2 function as Lewis acid sites for activating carbonyl groups (Fig. S12a), thereby facilitating the conversion of PCL-derived intermediates during reductive ammonolysis.[33] To probe the effect of oxygen-vacancy concentration on catalytic performance, Pt/TiO_2 was subjected to H_2 pre-reduction. Longer pre-reduction (0 h → 2 h → 6 h) strengthened the ESR oxygen vacancy signal, increased AZP yield (18% → 48% → 54%), and decreased CLA yield (24% → 11% → 8%), supporting the promoting effect of oxygen vacancies on the pathway toward AZP (Fig. S9). Furthermore, the presence of acid–base pair sites on the TiO_2 support is expected to play a crucial role in NH_3 activation (Fig. S12b).[34,35] Collectively, these features suggest that oxygen vacancies and acid–base pair sites on TiO_2 activate both carbonyl groups in PCL and NH_3, enabling effective PCL upcycling (Fig. 3).

To elucidate the depolymerization behavior of PCL and the reaction pathway, a combination of gel permeation chromatography (GPC) analysis, control experiments, and time-course studies was employed. GPC analysis showed that pristine PCL had number average molecular weight (M_n) and mass average molecular weight (M_w) values of 20.1 and 26.7 kg mol^{-1}, respectively, with a dispersity of 1.3. After the reaction over Pt/TiO_2, both M_n and M_w values significantly decreased (M_n: 5.6–6.4; M_w: 11.4–18.3), accompanied by a substantial increase in dispersity (2.0–2.8). These changes indicate that PCL depolymerization proceeded mainly *via* random chain scission rather than a chain-end unzipping process (Fig. S4).[15,36] On this basis, two plausible reaction paths to AZP were considered (Scheme 2): pathway A involving CLO and 6-hydroxyhexanamide, followed by CLA, and pathway B involving 1,6-hexanediol, followed by 6-aminohexanol. Time-course analysis revealed the sequential appearance of CLO and CLA, whereas no diol-derived intermediates were detected (Fig. 4), supporting pathway A as the dominant route to AZP. Complementarily, quantitative ^1H NMR of the water-soluble fraction revealed that 6-hydroxyhexanamide and 6-aminocaproic acid reach maximum yields at early reaction

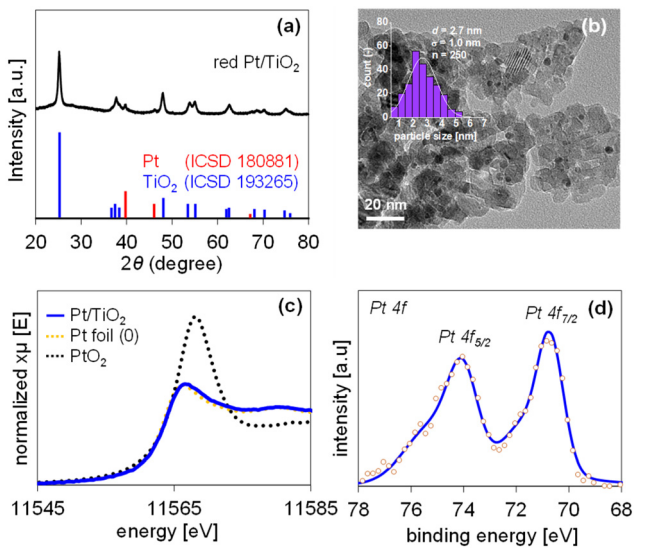

Fig. 2 (a) XRD pattern of reduced Pt/TiO_2. (b) TEM image and size distribution histogram (inset) of reduced Pt/TiO_2. (c) Pt L_3-edge XANES spectra of reduced Pt/TiO_2. (d) The XPS spectra in the Pt 4f region of Pt/TiO_2 (measured under air exposure).

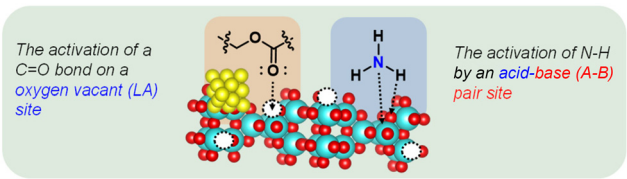

Fig. 3 Schematic illustration of dual activation on reduced Pt/TiO_2: oxygen vacancies activate C═O bonds, while acid–base pair sites facilitate N–H activation.

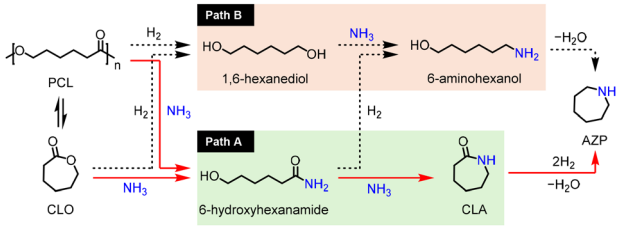

Scheme 2 The plausible reaction paths of PCL to AZP.

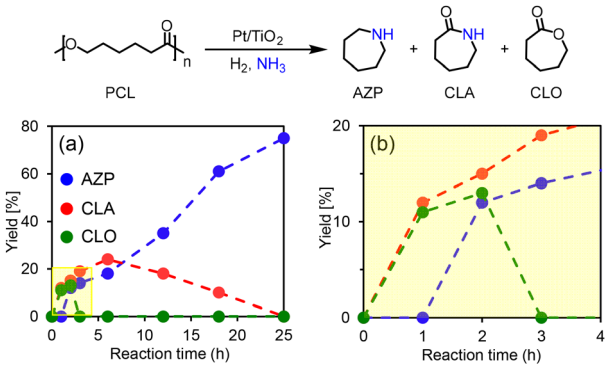

Fig. 4 [a] Time-course data of the Pt/TiO_2 catalysed reaction of PCL with NH_3 to produce AZP. [b] Initial four hours of the Pt/TiO_2 catalysed reaction of PCL with NH_3 to produce AZP. Reaction conditions: Pt/TiO_2 (8 mol% Pt), PCL (0.5 mmol), *n*-heptane (10 mL), NH_3 (0.7 MPa), H_2 (4 MPa), 180 °C, 25 h.

times and decrease thereafter, supporting their assignment as polar intermediates in the pathway to CLA (Fig. S2). Furthermore, these intermediates were examined through control experiments. CLO, 6-hydroxyhexanamide, and 6-aminocaproic acid primarily yielded CLA together with AZP (Table S4, entries 1, 3, and 4). Consistent with this assignment, CLA alone afforded AZP in 46% yield under the same conditions (Table S4, entry 2), establishing CLA as the key intermediate. Collectively, these results identify the CLO → 6-hydroxyhexanamide → 6-aminocaproic acid CLA → AZP sequence as the dominant pathway under Pt–TiO_2 catalysis.

Based on GPC analysis, time-course studies, control experiments, and structural characterization, a reaction pathway for the Pt/TiO_2-catalysed reductive ammonolysis of PCL was proposed (Scheme 3). Strong acid sites on Pt/TiO_2 promote early-stage depolymerization of PCL *via* random chain scission, as evidenced by GPC analysis, leading to enhanced CLO formation (Table 1 and Fig. S8). Ammonia incorporation occurs *via* TiO_2-assisted activation of the ester carbonyl group in CLO, resulting in the transient formation of 6-hydroxyhexanamide. Subsequent Pt-mediated hydrogen transfer and C–N bond reorganization are proposed to afford 6-aminocaproic acid under the reaction conditions (Fig. S2).[20,37,38] Subsequently, intramolecular cyclization affords CLA,[39] which is further converted to AZP through hydrogenation.[40,41] At this stage, this hydrogenation is governed by the cooperative interplay between C═O–O_v–TiO_2 interactions and metallic Pt^0 species.[33,42] Overall, the

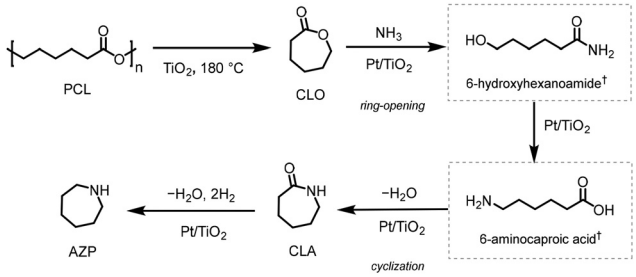

Scheme 3 Proposed reaction pathway for the Pt/TiO_2-catalysed reductive ammonolysis of PCL. (†) Undetectable under the present GC conditions.

cooperative catalysis between Pt nanoparticles and the TiO_2 support enables direct reductive ammonolysis of PCL to AZP.

Consistent with this mechanistic picture, the AZP yield declines upon extended reuse is best attributed to the nanoscale and surface evolution of the catalyst, whereas TEM and CHN reveal Pt particle growth and carbon accumulation (Tables S2, S3, Fig. S5 and S6). In this context, Pt 4f XPS points to a reduced surface contribution of metallic Pt^0 after cycling, consistent with a lower hydrogenation capacity upon extended reuse (Fig. S7). Detailed post-reaction characterization is provided in the SI.

Conclusions

In summary, this work reports the first direct upcycling of PCL into AZP using a Pt/TiO_2 catalyst. Under optimized conditions (Pt/TiO_2, 180 °C, 4.0 MPa H_2, 0.7 MPa NH_3, 25 h, heptane), PCL was converted to AZP in 75% yield. This approach avoids stoichiometric activation of reagents, producing water as the sole by-product and delivering a pharmaceutically relevant N-heterocycle. From a qualitative life-cycle perspective, these features are balanced by the current need for pressurized H_2/NH_3, which remains an important target for future improvement. Based on an AZP-only product boundary and assuming solvent recovery, the reaction exhibits an atom economy of 73% and an *E*-factor of 0.48. The reaction allows simple catalyst recovery and reuse. The transformation is enabled by cooperative catalysis between Pt and the TiO_2 support, which integrates depolymerization, nitrogen incorporation, and hydrogenation into a single sequence. This work establishes a foundation for plastic upcycling to value-added nitrogen-containing heterocycles within the framework of green and sustainable chemistry.

Author contributions

D. P. and S. Y. designed the experiments. D. P. and Y. T. conducted the catalytic activity tests and characterized the catalysts. K. S., T. Mit. and T. Miz. discussed the experiments and results. D. P. and S. Y. wrote the manuscript with

input from all the authors. All authors commented critically on the manuscript and approved the final manuscript.

Conflicts of interest

There are no conflicts to declare.

Data availability

The supporting data have been provided as part of the supplementary information (SI). Supplementary information is available. See DOI: https://doi.org/10.1039/d6gc00098c.

Acknowledgements

This work was supported by JSPS KAKENHI (Grant No. 21K04776, 23H01761 and 24K01255) and Daicel-Engineering Science Collaborative Laboratory, which was established by Daicel Corporation and the Graduate School of Engineering Science, the University of Osaka. This study was partially supported by JST-CREST (Grant No. JPMJCR21L5), the Cooperative Research Program of the Institute for Catalysis, Hokkaido University (Grant No. 23DS0434a), and Dana PNBP FMIPA, Universitas Negeri Malang (5.4.50/UN32.3.2/LT/2021). K. S. is thankful for a JSPS Research Fellowship for Young Scientists (grant number 23KJ1473). A part of the experimental analysis (NMR, ESR, XPS, ICP-AES, and CHN EA) was supported by the Advanced Research Infrastructure (Program for supporting construction of core facilities, Grant No. JPMXS0441200025) of the Ministry of Education, Culture, Sports, Science, and Technology (MEXT), Japan. The authors also thank Dr Yuichiro Kobayashi at the Graduate School of Science, the University of Osaka, for the GPC measurement.

References

1 K. Houssini, J. Li and Q. Tan, *Commun. Earth Environ.*, 2025, **6**, 257.
2 R. C. Hale, A. E. King, J. M. Ramirez, M. La Guardia and C. Nidel, *Environ. Sci. Technol. Lett.*, 2022, **9**, 798–807.
3 M. Jin, M. Sun, J. Liu, C. Dong and J. Xue, *Sci. Total Environ.*, 2024, **912**, 169347.
4 E. Smith, M. M. Bilec and V. Khanna, *ACS Sustainable Chem. Eng.*, 2023, **11**, 2055–2065.
5 C. Gioia, G. Giacobazzi, M. Vannini, G. Totaro, L. Sisti, M. Colonna, P. Marchese and A. Celli, *ChemSusChem*, 2021, **14**, 4167–4175.
6 S. T. R. Velasquez, Q. Hu, J. Kramm, V. C. Santin, C. Völker and F. R. Wurm, *Angew. Chem., Int. Ed.*, 2025, **64**, e202423406.
7 C. Shi, E. C. Quinn, W. T. Diment and E. Y.-X. Chen, *Chem. Rev.*, 2024, **124**, 4393–4478.
8 T. Uekert, A. Singh, J. S. DesVeaux, T. Ghosh, A. Bhatt, G. Yadav, S. Afzal, J. Walzberg, K. M. Knauer, S. R. Nicholson, G. T. Beckham and A. C. Carpenter, *ACS Sustainable Chem. Eng.*, 2023, **11**, 965–978.
9 C. Jehanno, J. W. Alty, M. Roosen, S. De Meester, A. P. Dove, E. Y.-X. Chen, F. A. Leibfarth and H. Sardon, *Nature*, 2022, **603**, 803–814.
10 M. Anwar, M. E. Konnova and S. Dastgir, *RSC Sustainability*, 2025, **3**, 3724–3840.
11 I. Vollmer, M. J. F. Jenks, M. C. P. Roelands, R. J. White, T. van Harmelen, P. de Wild, G. P. van der Laan, F. Meirer, J. T. F. Keurentjes and B. M. Weckhuysen, *Angew. Chem., Int. Ed.*, 2020, **59**, 15402–15423.
12 H. Luo, H. Tyrrell, J. Bai, R. I. Muazu and X. Long, *Green Chem.*, 2024, **26**, 11444–11467.
13 N. Raina, R. Pahwa, J. K. Khosla, P. N. Gupta and M. Gupta, *Polym. Bull.*, 2022, **79**, 7041–7063.
14 J. Su, G. Xu, B. Dong, R. Yang, H. Sun and Q. Wang, *Polym. Chem.*, 2022, **13**, 5897–5904.
15 C. F. Gallin, W.-W. Lee and J. A. Byers, *Angew. Chem., Int. Ed.*, 2023, **62**, e202303762.
16 E. Cheung, C. Alberti, S. Bycinskij and S. Enthaler, *ChemistrySelect*, 2021, **6**, 8063–8067.
17 C. Alberti and S. Enthaler, *ChemistrySelect*, 2021, **6**, 11244–11248.
18 T. Urayama, A. Watanabe and R. Miyazaki, *JP Patent*, JP7123002, 2022.
19 F. Poovan, R. V. Jagadeesh and M. Beller, *Chem*, 2026, **12**, 102667.
20 H. Zhang, Y. Zhao, Y. Wang, R. Li, M. Tang, W. Zeng, Y. Wang, X. Chang, B. Han and Z. Liu, *Green Chem.*, 2024, **26**, 3159–3164.
21 Y. Wang, H. Zhang, W. Zeng, Y. Zhao, R. Li, M. Tang, B. Han and Z. Liu, *Angew. Chem., Int. Ed.*, 2025, **64**, e202424236.
22 K. E. O. Ylijoki and J. M. Stryker, *Chem. Rev.*, 2013, **113**, 2244–2266.
23 T. Liu, Y. Fang, L. Zuo, Y. Yang, Y. Liu, W. Chen, L. Dang and W. Guo, *Org. Chem. Front.*, 2021, **8**, 1902–1909.
24 R. Mykura, R. Sánchez-Bento, E. Matador, V. K. Duong, A. Varela, L. Angelini, R. J. Carbajo, J. Llaveria, A. Ruffoni and D. Leonori, *Nat. Chem.*, 2024, **16**, 771–779.
25 G.-F. Zha, K. P. Rakesh, H. M. Manukumar, C. S. Shantharam and S. Long, *Eur. J. Med. Chem.*, 2019, **162**, 465–494.
26 A. Lewera, L. Timperman, A. Roguska and N. Alonso-Vante, *J. Phys. Chem. C*, 2011, **115**, 20153–20159.
27 Z. Luo, X. Han, Z. Ma, B. Zhang, X. Zheng, Y. Liu, M. Gao, G. Zhao, Y. Lin, H. Pan and W. Sun, *Angew. Chem., Int. Ed.*, 2024, **63**, e202406728.
28 Z. Liu, B. Jia, Y. Zhang and M. Haneda, *Ind. Eng. Chem. Res.*, 2020, **59**, 13916–13922.
29 L. Li, P. Wu, Q. Yu, G. Wu and N. Guan, *Appl. Catal., B*, 2010, **94**, 254–262.
30 F. Amano, M. Nakata, A. Yamamoto and T. Tanaka, *J. Phys. Chem. C*, 2016, **120**, 6467–6474.
31 M. Y. Byun, Y. E. Kim, J. H. Baek, J. Jae and M. S. Lee, *RSC Adv.*, 2022, **12**, 860–868.

32 Y. Zou, X. Li, Y. Zhao, X. Liu, S. Xie, F. Liu and T. Zhu, *ACS Catal.*, 2025, **15**, 6346–6360.
33 S. Huygh, A. Bogaerts and E. C. Neyts, *J. Phys. Chem. C*, 2016, **120**, 21659–21669.
34 A. A. Tsyganenko, D. V. Pozdnyakov and V. N. Filimonov, *J. Mol. Struct.*, 1975, **29**, 299–318.
35 T. Tsuda, H. Ishikawa, M. Sheng, M. Hirayama, S. Suganuma, R. Osuga, K. Nakajima, J. N. Kondo, S. Yamaguchi, T. Mizugaki and T. Mitsudome, *J. Am. Chem. Soc.*, 2025, **147**, 14326–14335.
36 G. R. Jones, H. S. Wang, K. Parkatzidis, R. Whitfield, N. P. Truong and A. Anastasaki, *J. Am. Chem. Soc.*, 2023, **145**, 9898–9915.
37 M. H. S. A. Hamid, P. A. Slatford and J. M. J. Williams, *Adv. Synth. Catal.*, 2007, **349**, 1555–1575.
38 M. Sarno, C. Cirillo and M. Iuliano, *ChemistryOpen*, 2019, **8**, 520–531.
39 C. Zhai, Z. Ma and Y. Wang, *Res. Chem. Intermed.*, 2024, **50**, 3821–3841.
40 J. R. Cabrero-Antonino, R. Adam, V. Papa and M. Beller, *Nat. Commun.*, 2020, **11**, 3893.
41 H. Yang, H. Garcia and C. Hu, *Green Chem.*, 2024, **26**, 2341–2364.
42 T. Mitsudome, K. Miyagawa, Z. Maeno, T. Mizugaki, K. Jitsukawa, J. Yamasaki, Y. Kitagawa and K. Kaneda, *Angew. Chem., Int. Ed.*, 2017, **56**, 9381–9385.

